Remedial Operation of a Fault-Tolerant Flux-Switching Permanent Magnet Motor for Electric Vehicle Applications

Wenxiang Zhao[1, 2], Ming Cheng[1], Wei Hua[1], Hongyun Jia[1], Ruiwu Cao[1], and Wei Wang[1]
[1]School of Electrical Engineering, Southeast University, Nanjing, China
[2]School of Electrical and Information Engineering, Jiangsu University, Zhenjiang, China
mcheng@seu.edu.cn

***Abstract*-Fault-tolerant flux-switching permanent magnet (FT-FSPM) motor is a new class of stator-PM brushless motors, a potential candidate for many applications where reliability and power density are of importance. In this paper, a new method is proposed for torque ripple minimization, in which the key is to introduce harmonic currents to compensate for non-ideal sinusoidal back-EMF. Moreover, a fault-tolerant control strategy is investigated, in which the effect of harmonic back-EMF is considered. Both simulation and experimental results confirm that the proposed control algorithms can reduce torque ripple under open-circuit fault conditions.**

I. INTRODUCTION

Fault-tolerance of motor drives is extremely important for some applications. Automotive, aerospace, naval, medical and military applications now incorporate a number of motor drives in such a way that the whole system relies heavily upon them [1]. Therefore, the development of fault-tolerant motor drives has received a great attention [2].

Previous research by a variety of authors has been carried out on the concepts, development, building, and testing of fault-tolerant motor drives for high reliability applications. The switched reluctance (SR) motors have gained attention due to their rugged construction and fault-tolerant capability [3]. In [4] and [5], some intelligent control strategies were proposed to improve the torque performance of a SR motor drive under fault conditions. In [6], fault analysis was performed and remedial strategy was proposed for fault-tolerant operation of SR motor drives. However, such motors are not desirable in many applications due to their low power density. Permanent magnet (PM) brushless motor drives have gained attention for a wide variety of applications due to their high power density and high efficiency [7]. A fault-tolerant brushless machine having PMs in the rotor (the so-called rotor-PM brushless machines) was proposed in [8]. In [9] and [10], some compensation techniques for open-circuited fault were proposed to improve the fault-tolerant performance of multiphase rotor-PM brushless motor drives. Nevertheless, it should be noted that these rotor-PM brushless motor drives inherently suffer from the problem of poor thermal dissipation in the rotor [2], which adversely affects the characteristics of PMs and hence the reliability of motor drives.

In recent years, a new class of brushless machines with PMs located in the stator, namely so-called stator-PM machines, has been proposed, offering high power density and good mechanical integrity [1],[7],[11]. Doubly-salient PM (DSPM) and flux-switching PM (FSPM) machines are both stator-PM machines, and have attracted considerably attention. It has been identified that a DSPM motor can inherently offer fault-tolerance [12],[13] and that the torque capability of a FSPM motor is significantly higher than that of a DSPM motor [14]-[16]. However, the mutual inductance of FSPM motors is higher than that of DSPM motors, which decreases fault-tolerant ability. Hence, how to improve the fault-tolerance capability of FSPM motors has attracted more and more attention. Very recently, a new FSPM motor with alternative wound teeth, termed as FT-FSPM motor, was proposed, which offers fault-tolerance, high power density and good mechanical integrity [17]. However, the back-EMF of FT-FSPM motor is asymmetric, resulting in undesired high torque ripple. Also, a rotor-skewing method was adopted to achieve a more sinusoidal back-EMF in [17], resulting in unfavorable increased manufacturing and reduced efficiency and power density.

Hence, the purpose of this paper is to propose new control strategies for normal and fault-tolerant operations of the new stator-PM fault-tolerant machines for minimizing torque ripple. In Section II, the FT-FSPM machine and its features will be briefly described. The harmonic analysis of back-EMF will be performed. In Section III, the operating principle by optimum harmonic current injection will be proposed, considering the influence of second-order harmonic back-EMF. In Section IV, computer simulations will be carried out to examine the proposed control strategies for FT-FSPM motor under normal and open-circuit fault conditions. Then, in Section V, experimental results will be used to verify the operations of the proposed method. Finally, conclusions will be drawn in Section VI.

This work was supported in part by grants (Project No. 60974060, 50907031 and 50807007) from the National Natural Science Foundation of China and Professional Research Foundation for Advanced Talents of Jiangsu University.

978-1-4244-8218-4/10/$26.00 ©2010 IEEE

II. STRUCTURE AND FEATURES

Fig. 1 shows a 3-phase 12-slot/10-pole FT-FSPM motor having 12 salient poles, e.g., 6 armature-teeth and 6 fault-tolerant-teeth, in the stator and 10 salient poles in the rotor. Since there are no PMs, brushes, nor windings in the rotor, the FT-FSPM motor exhibits the advantages of simple rotor configuration and mechanical robustness. On the other hand, due to the location of the magnets in the stator, rather than rotor as in the conventional rotor-PM motors, the FT-FSPM motor can eliminate the problem of cooling difficulty and mechanical instability, and retain the merits of high efficiency and high power density. Since the phase windings are essentially isolated by using fault-tolerant-teeth, magnetically, thermally and physically, fault tolerance of a FSPM motor has significantly enhanced. Fig. 2 compares the inductance characteristics of FT-FSPM and conventional FSPM motor, illustrating that the ratio of the mutual to the self inductances in the conventional FSPM motor is nearly six times that in FT-FSPM motor. The predicted back-EMF waveforms are shown in Fig. 3 and the harmonics analysis of the back-EMF waveforms are shown in Fig. 4. It can be seen that the back-EMF of FT-FSPM motor has rich harmonic components.

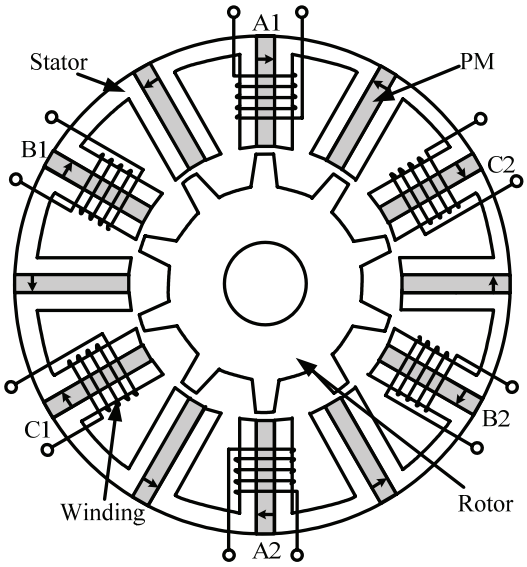

Fig. 1. Cross-section of FT-FSPM motor.

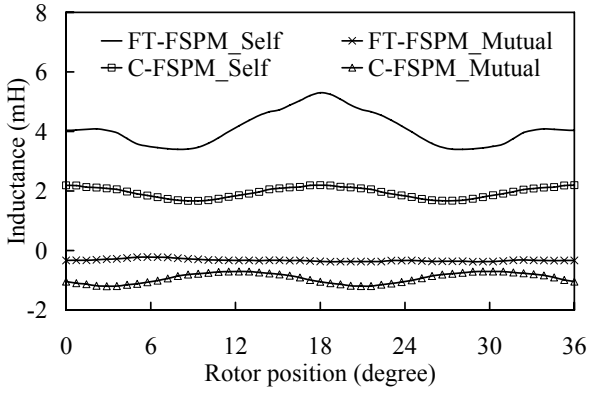

Fig. 2. Comparison of inductance.

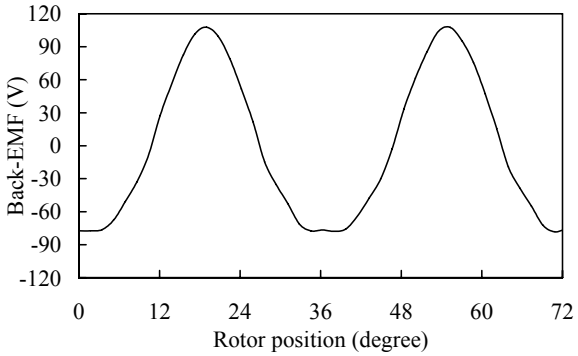

Fig. 3. Predicted back-EMF waveform.

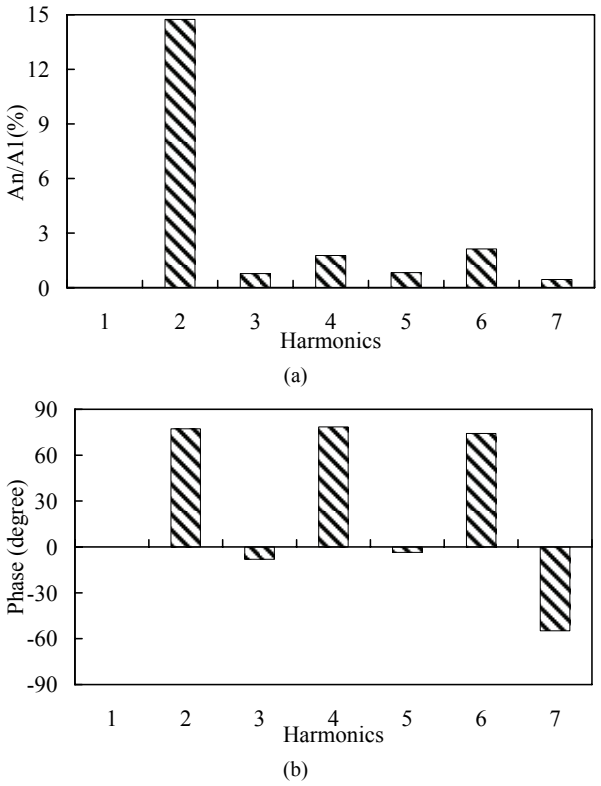

Fig. 4. Harmonics analysis of predicted back-EMF. (a) Normalized magnitude. (b) Phase angle.

III. CONTROL STRATEGY

It confirms that the harmonic components of back-EMF result in higher torque ripple than the conventional FSPM motor [16]. For the conventional FSPM motor, the back-EMF waveform is ideal sinusoidal. When the current controller of the motor drive system is required to track a set of sinusoidal current, the resulting torque should be free from ripples. However, a FT-FSPM motor cannot produce the ideal sinusoidal back-EMF waveform. So, when the motor operates in brushless AC (BLAC) mode, the resulting torque is contaminated with ripples. The characteristics of average torque and torque ripple versus the peak phase current of the FT-FSPM motor are calculated by using finite element method and plotted together as shown in Fig. 5.

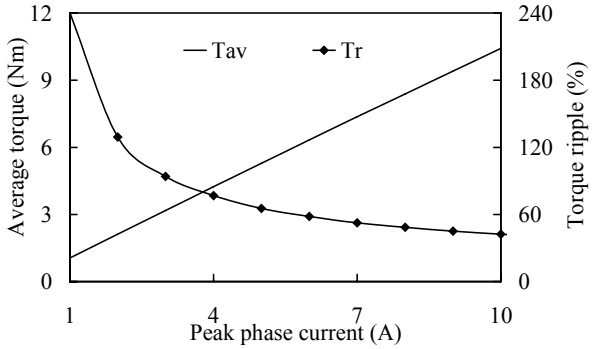

Fig. 5. Average torque and torque ripple.

In this work, the proposed torque ripple minimization is to online shape the armature current waveform. Optimal amplitude of the injected current to minimize torque ripple is derived as a function of the injected current.

A. Normal Operation

It can be known from the harmonics analysis of the back-EMF that the most significant component is the second-order harmonic, higher order harmonics being relatively low. Neglecting the influence of the higher order harmonics, the back-EMFs of the FT-FSPM motor can be expressed as:

$$\begin{cases} e_a = e_{a1} + e_{a2} = E_1 \sin(\omega t) + E_2 \sin(2\omega t + \varphi) \\ e_b = e_{b1} + e_{b2} = E_1 \sin(\omega t + 2\pi/3) \\ \quad + E_2 \sin[2(\omega t + 2\pi/3) + \varphi] \\ e_c = e_{c1} + e_{c2} = E_1 \sin(\omega t - 2\pi/3) \\ \quad + E_2 \sin[2(\omega t - 2\pi/3) + \varphi] \end{cases} \quad (1)$$

where ω is the frequency of the fundamental component, φ is the second-order harmonic angle relative to fundamental phase, and E_1 and E_2 are the amplitude of the fundamental and the second-order harmonic back-EMF, respectively.

To offset the effect of the second-order harmonic of back-EMF, the optimal harmonic currents at normal operation are assumed as:

$$\begin{cases} i_a = I_1 \sin(\omega t) + I_2 \sin(2\omega t + \gamma) \\ i_b = I_1 \sin(\omega t + 2\pi/3) + I_2 \sin[2(\omega t + 2\pi/3) + \gamma] \\ i_c = I_1 \sin(\omega t - 2\pi/3) + I_2 \sin[2(\omega t - 2\pi/3) + \gamma] \end{cases} \quad (2)$$

where I_1 and I_2 are the maximum value of the fundamental and the second-order harmonic phase current, respectively. So, the total electromagnetic torque T_n can be expressed as:

$$\begin{aligned} T_n &= (e_a \cdot i_a + e_b \cdot i_b + e_c \cdot i_c)/\omega \\ &= (3/2\omega) \cdot [E_1 I_1 + E_1 I_2 \cos(3\omega t + \gamma) \\ &\quad + E_2 I_1 \cos(3\omega t + \varphi) + E_2 I_2 \cos(\varphi - \gamma)] \end{aligned} \quad (3)$$

Since the electromagnetic torque does not vary with rotor position and keeps constant, the following relations are selected as:

$$\begin{cases} \gamma = \varphi \\ E_1 I_2 = -E_2 I_1 \end{cases} \quad (4)$$

It can be known from harmonic analysis of back-EMF shown in Fig. 3:

$$\begin{cases} \varphi = -2\pi/5 \\ E_2 = 0.15 E_1 \end{cases} \quad (5)$$

Then, by using (2), (4) and (5), the optimal harmonic current at normal operation is achieved as:

$$\begin{cases} i_a = I_1[\sin(\omega t) - 0.15\sin(2\omega t - 2\pi/5)] \\ i_b = I_1[\sin(\omega t + 2\pi/3) - 0.15\sin(2\omega t + 14\pi/15)] \\ i_c = I_1[\sin(\omega t - 2\pi/3) - 0.15\sin(2\omega t + 4\pi/15)] \end{cases} \quad (6)$$

B. Fault-Tolerant Operation

In case the motor drive is under fault, the faulty phase can be shut off and the remaining phases can continue operation. Thus, proper fault detectors need to be employed. Detailed discussions on the fault detectors for motor drives have been studied in [18] and [19]. This work focuses on how to develop a remedial control method to improve the torque performance of FT-FSPM motor drives under the open-circuit fault.

By substituting (4) into (3), the total electromagnetic torque under normal condition is calculated as:

$$T_N = 1.48 E_1 I_1 \quad (7)$$

When phase-A is open-circuited, the current in phase-A drops to zero and the electromagnetic torque will be the torque sum of phases-B and -C, i.e.,

$$T_f = (e_b \cdot i_b' + e_c \cdot i_c')/\omega \quad (8)$$

After this fault occurs, the same torque may be obtained when (7) is equated to (4), and then the remedial currents of the healthy phases are assumed to be:

$$\begin{cases} i_a' = 0 \\ i_b' = \dfrac{1.48 E_1 I_1 (e_{b1} - e_{b2})}{(e_{b1}^2 + e_{c1}^2) - (e_{b2}^2 + e_{c2}^2)} \\ i_c' = \dfrac{1.48 E_1 I_1 (e_{c1} - e_{c2})}{(e_{b1}^2 + e_{c1}^2) - (e_{b2}^2 + e_{c2}^2)} \end{cases} \quad (9)$$

Substituting (1) and (4) to (9), the remedial currents are derived as:

$$\begin{cases} i_a' = 0 \\ i_b' = I_1 \cdot \dfrac{1.48\sin(\omega t + 2\pi/3) - 0.21\sin(2\omega t + 14\pi/15)}{0.98 + 0.5\cos(2\omega t) - 0.01\cos(4\omega t - 4\pi/5)} \\ i_c' = I_1 \cdot \dfrac{1.48\sin(\omega t + 2\pi/3) - 0.21\sin(2\omega t + 4\pi/15)}{0.98 + 0.5\cos(2\omega t) - 0.01\cos(4\omega t - 4\pi/5)} \end{cases} \quad (10)$$

By neglecting the fourth-order harmonic current, the current expression can be simplified as:

$$\begin{cases} i_a' = 0 \\ i_b' = I_1 \cdot \dfrac{2.96\sin(\omega t + 2\pi/3) - 0.42\sin(2\omega t + 14\pi/15)}{1.96 + \cos(2\omega t)} \\ i_c' = I_1 \cdot \dfrac{2.96\sin(\omega t - 2\pi/3) - 0.42\sin(2\omega t + 4\pi/15)}{1.96 + \cos(2\omega t)} \end{cases} \quad (11)$$

IV. SIMULATION

To quantitatively evaluate the performances of the FT-FSPM motor drive at various operations, the average torque value and the torque ripple level are useful. So, the torque ripple factor is defined as:

$$K_T = \frac{T_{max} - T_{min}}{T_{av}} \times 100\% \quad (12)$$

where T_{max}, T_{min} and T_{av} are the maximum, the minimum and the average values of the output torque, respectively.

Under normal condition, the FT-FSPM motor drive operates in the conventional BLAC mode. The motor current and torque waveforms are obtained as shown in Fig. 6. It can be seen the current waveform is sinusoidal and the FT-FSPM motor suffers from severe torque ripples.

To minimize the torque ripple, second-order harmonic current is injected. The simulated current and torque waveforms are shown in Fig. 7. In contrast, when adopting the harmonic current injection control, the FT-FSPM motor produces smooth torque. It can be found that the calculated K_t is significantly reduced from 34.5% to 11.7%.

In the event of the open-circuit fault, the proposed remedial operation is activated. In order to verify that the aforementioned harmonic fault-tolerant operation can continue the motor operation, the current and torque waveforms are simulated by using (11). As shown in Fig. 8, the calculated K_t is 28.3%. It should be noted that the torque ripple is caused by unbalanced operation and the higher order harmonics of back-EMF. However, it can be seen that there is no existence of torque dead zone. Thus, the proposed remedial strategy insures that the performance of faulty operation has been enhanced, slightly inferior to that of proposed normal operation.

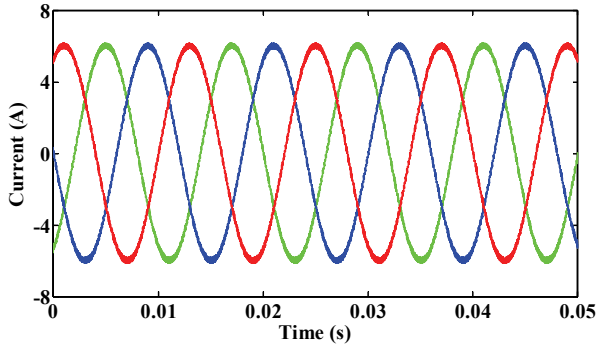

(a)

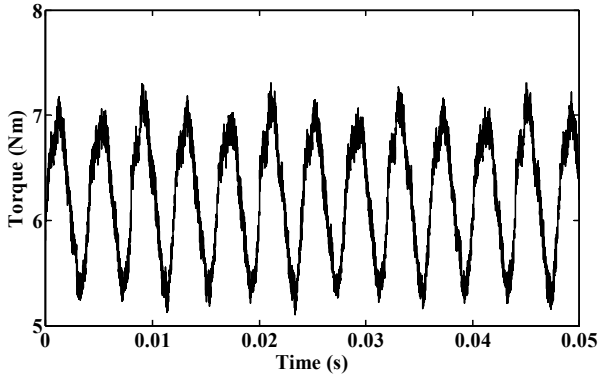

(b)

Fig. 6. Waveforms at conventional BLAC operation. (a) Current. (b) Torque.

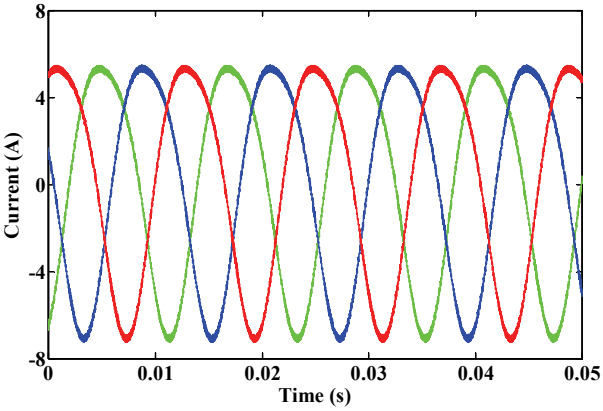

(a)

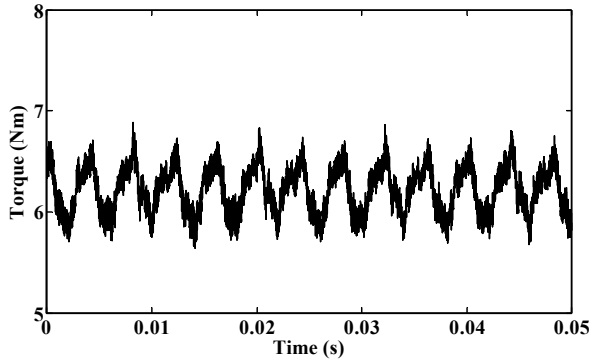

(b)

Fig. 7. Waveforms at proposed normal operation. (a) Current. (b) Torque.

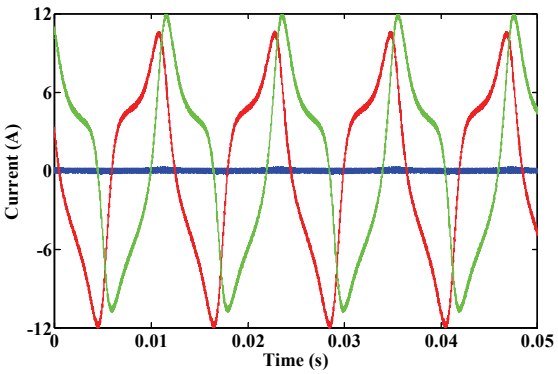

(a)

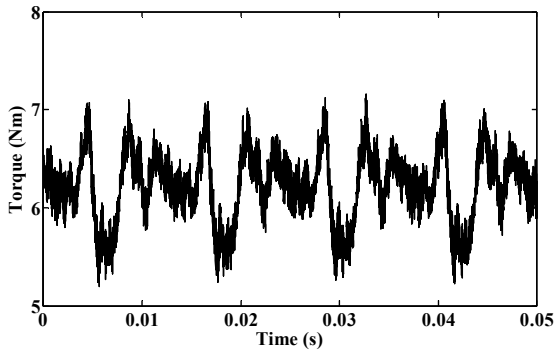

(b)

Fig. 8. Waveforms at proposed fault-tolerant operation. (a) Current. (b) Torque.

V. EXPERIMENTAL RESULTS

A 3-phase FT-FSPM motor has been designed and manufactured for verification, as shown in Fig. 9. Also, an IPM-based converter and a DSP-based digital controller are built to drive the experimental motor. A separately excited dc generator is mechanically coupled to the prototype motor, and works as variable mechanical load.

Firstly, the FT-FSPM motor drive operates in the normal mode. The measured back-EMF waveform is shown in Fig. 10, and its harmonics analysis result is shown in Fig. 11. It can be found that the back-EMF waveform is not ideal sinusoidal and contains higher-order harmonics, which agrees with the theoretical one shown in Fig. 3. Meanwhile, the measured current waveforms are shown in Fig. 11(a). As expected, these current waveforms are with second-order harmonic current injection, which agree with the theoretical one shown in Fig. 7(a). During the open-circuit fault with the loss of one phase, the FT-FSPM motor drive operates in the remedial harmonic mode. The measured current waveforms are shown in Fig. 12(b). It can be seen that the current waveforms of the two healthy phases are fed by harmonic currents, which agree with the theoretical ones as shown in Fig. 8(a).

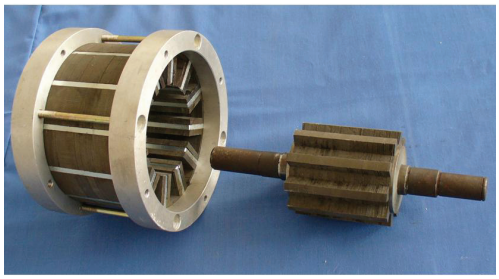

Fig. 9. Prototype machine. (a) Stator. (b) Rotor.

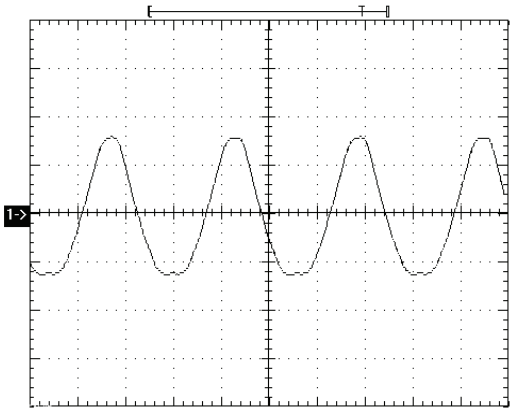

Fig. 10. Measured back-EMF waveform (1 ms/div, 50 V/div).

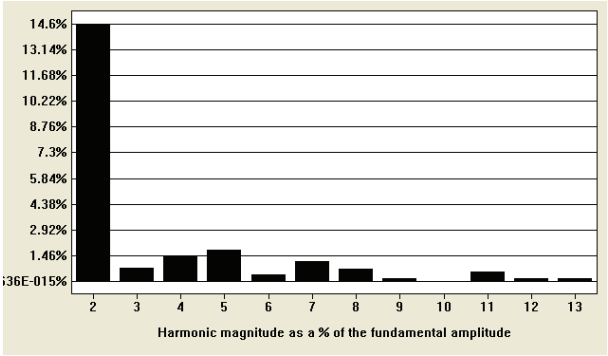

Fig. 11. Harmonics analysis of measured back-EMF.

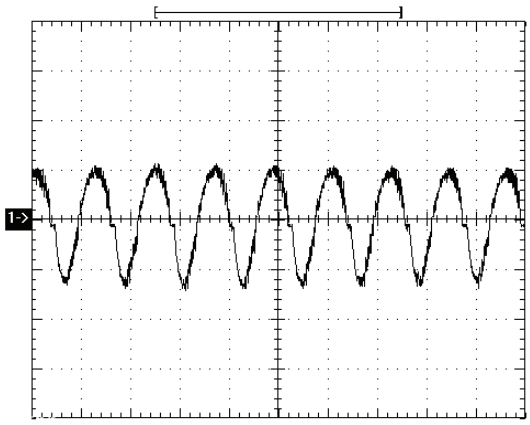

(a)

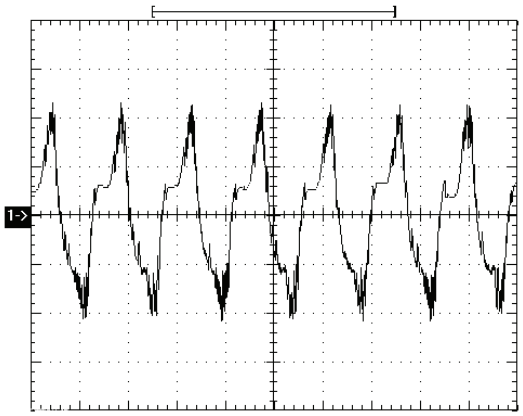

(b)

Fig. 12. Measured current waveforms at proposed operations (5 ms/div, 3 A/div). (a) Normal condition. (b) Fault-tolerant condition.

VI. CONCLUSION

This paper has proposed a new control strategy for stator-PM fault-tolerant motors having asymmetric back-EMFs, with the aim to minimize torque ripple under normal and faulty conditions. By using harmonics analysis of the back-EMF, the second-order harmonics currents are employed to improve torque smoothness. Both the theoretical and experimental results have shown that the proposed method can reduce torque ripple, and it is possible to maintain balanced operation when the FT-FSPM machine is met with open-circuited fault. This remedial operation is particularly important to enable fault tolerance for many practical applications such as electric vehicle.

REFERENCES

[1] Z. Q. Zhu and D. Howe, "Electrical machines and drives for electric, hybrid, and fuel cell vehicles," *IEEE Proc.*, vol. 95, no. 4, pp. 746-765, Apr. 2007.

[2] B. A. Welchko, T. A. Lipo, T. M. Jahns, and S. E. Schulz, "Fault tolerant three-phase ac motor drive topologies: a comparison of features, cost, and limitations," *IEEE Trans. Power Electron*., vol. 19, no. 4, pp. 1108-1116, Jul. 2004.

[3] C. M. Stephens, "Fault detection and management system for fault-tolerant switched reluctance motor drives," *IEEE Trans. Ind. Appl.*, vol. 27, no. 6, pp. 1098-1102, Nov./Dec. 1991.

[4] L. A. Belfore II and A. Arkadan, "A methodology for characterizing fault tolerant switched reluctance motors using neurogenetically derived models," *IEEE Trans. Energy Convers*., vol. 17, no. 3, pp. 380-384, Sep. 2002.

[5] S. Mir, M. S. Islam, T. Sebastian, and I. Husain, "Fault tolerant switched reluctance motor drive using adaptive fuzzy logic controller," *IEEE Trans. Power Electron*., vol. 19, no. 2, pp. 289-295, Mar. 2004.

[6] S. Gopalakrishnan, A. M. Omekanda, and B. Lequesne, "Classification and remediation of electrical faults in the switched reluctance drive," *IEEE Trans. Ind. Appl*., vol. 42, no. 2, pp. 479-486, Mar./Apr. 2006.

[7] K. T. Chau, C. C. Chan, and C. Liu, "Overview of permanent-magnet brushless drives for electric and hybrid electric vehicles," *IEEE Trans. Ind. Electron*., vol. 55, no. 6, pp. 2246-2257, Jun. 2008.

[8] A. G. Jack, B. C. Mecrow, and J. Haylock, "A comparative study of PM and SR motors for high performance fault tolerant applications," *IEEE Trans. Ind. Appl.* vol. 32, no. 4, pp. 889-895, Jul./Aug. 1996.

[9] L. Parsa and H. A. Toliyat, "Fault-tolerant interior-permanent-magnet machines for hybrid electric vehicle applications," *IEEE Trans. Veh. Technol.* vol. 56, no. 4, pp. 1546-1552, Jul. 2007.

[10] S. Dwari and L. Parsa, "An optimal control technique for multiphase PM machines under open-circuit faults," *IEEE Trans. Ind. Electron*., vol. 55, no. 5, pp. 1988-1995, May 2008.

[11] M. Cheng, W. Hua, X. Zhu, X. Kong, J. Zhang, and W. Zhao, "Stator-permanent magnet brushless machines: concepts, developments and applications," in *Proc. 2008 Int. Conf. Electr. Mach. Syst.*, pp. 2802-2807.

[12] W. Zhao, M. Cheng, X. Zhu, W. Hua, and X. Kong, "Analysis of fault-tolerant performance of a doubly salient permanent-magnet motor drive using transient cosimulation method," *IEEE Trans. Ind. Electron.*, vol. 55, no. 4, pp. 1739-1748, Apr. 2008.

[13] W. Zhao, K. T. Chau, M. Cheng, J. Hi, and X. Zhu, "Remedial brushless AC operation of fault-tolerant doubly-salient permanent-magnet motor drives," *IEEE Trans. Ind. Electron.*, vol. 57, no. 6, pp. 2134-2141, Jun. 2010.

[14] Z. Q. Zhu, Y. Pang, D. Howe, S. Iwasaki, R. Deodhar, and A. Pride "Analysis of electromagnetic performance of flux-switching permanent-magnet machines by nonlinear adaptive lumped parameter magnetic circuit model," *IEEE Trans. Magn.,* vol. 41, no.11, pp. 4277-4287, Nov. 2005.

[15] W. Hua, M. Cheng, H. Jia, and X. Fu, "Comparative study of flux-switching and doubly-salient PM machines particularly on torque capability," in *Conf. Rec. 2008 IEEE-IAS Annu. Meet.*, pp. 1-8.

[16] W. Zhao, M. Cheng, W. Hua, H. Jia, and R. Cao "Back-EMF harmonic analysis and fault-tolerant control of flux-switching permanent-magnet machine with redundancy," *IEEE Trans. Ind. Electron.*, in press.

[17] R. L. Owen, Z. Q. Zhu, A. S. Thomas, G. W. Jewell and D. Howe, "Alternate Poles Wound Flux-Switching Permanent-Magnet Brushless AC Machines," *IEEE Trans. Ind. Appl*., vol. 46, no. 2, pp. 790-797, Mar./Apr. 2010.

[18] O. Poncelas, J. A. Rosero, J. Cusido, J. A. Ortega, and L. Romeral, "Motor fault detection using a Rogowski sensor without an integrator," *IEEE Trans. Ind. Electron*., vol. 56, no. 10, pp. 4062-4070, Oct. 2009.

[19] S. A. Arogeti, D. Wang, C. B. Low, "Mode identification of hybrid systems in the presence of fault," *IEEE Trans. Ind. Electron*., vol. 57, no. 4, pp. 1452-1467, Apr. 2010.

Wenxiang Zhao was born in Jilin, China, in 1976. He received the B.Sc. and M.Sc. degrees in electrical engineering from Jiangsu University, Zhenjiang, China, in 1999 and 2003, respectively, and the Ph.D. degree in electrical engineering at Southeast University, Nanjing, China, in 2010.

Ming Cheng received the B.Sc. and M.Sc. degrees from the Department of Electrical Engineering, Southeast University, China, in 1982 and 1987, respectively, and Ph.D. degree from the Department of Electrical and Electronic Engineering, The University of Hong Kong, Hong Kong, in 2001.

Wei Hua was born in 1978, in Jiangsu, China. He received the B.Sc. and Ph.D degrees in 2001 and 2007, respectively, from Southeast University, Nanjing, China, both in electrical engineering.

Hongyun Jia was born in Henan, China, in 1979. She received the B.Sc. degree in electrical and information engineering from Xinyang Normal University, Xinyang, China, in 2003, and M.Sc. degrees in electrical engineering from Jiangsu University, Zhenjiang, China, in 2006. She is currently working toward the Ph.D. degree in electrical engineering at Southeast University, Nanjing, China.

Ruiwu Cao was born in Jiangsu, China, in 1980. He received the B.Sc. degree in electrical engineering from Yancheng Institute of Technology, Yancheng, China, in 2004, and the M.Sc. degree in electrical engineering from Southeast University, Nanjing, China, in 2007. He is currently working toward the Ph.D. degree in electrical engineering at Southeast University, Nanjing, China.

Wei Wang was born in Jiangsu, China, in 1986. He received the B.Sc. degree in electrical engineering from Nanjing University of Science and Technology, Nanjing, China, in 2008. He is currently working toward the Ph.D. degree at Southeast University, Nanjing, China.